water

MDPI

Article

Impact of Climate Change on Portuguese Marine Coastal Environments

Miguel Pinto [1,*], Juan Bueno-Pardo [2], Martinho Marta-Almeida [3,4] and Francisco Leitão [1,*]

[1] Centro de Ciências do Mar do Algarve (CCMAR/CIMAR LA), Campus de Gambelas, Universidade do Algarve, 8005-139 Faro, Portugal
[2] Centro de Investigación Mariña (CIM), Universidade de Vigo, Future Oceans Lab, Campus Lagoas Marcosende, 36310 Vigo, Spain; jbuenopardo@gmail.com
[3] Centro de Estudos de Ambiente e Mar, Departamento de Biologia, Universidade de Aveiro, 3810-193 Aveiro, Portugal
[4] Grupo de Oceanografia Tropical, Universidade Federal da Bahia, Salvador 40170-115, Brazil
* Correspondence: mfpinto@ualg.pt (M.P.); fleitao@ualg.pt (F.L.)

Abstract

The potential impacts of climate change on marine habitats were assessed using RCP4.5 and RCP8.5 projections of environmental parameters that included sea surface temperature (SST), pH, salinity, planktonic productivity (PP) and current strength (CS). The analysis was conducted separately for three distinct oceanographic regions of the Portuguese coastline (North, Centre and South) up to the middle of the century. Temporal trends in environmental variables were assessed using time series analyses. Overall, changes expected up to the middle of the century include increasing SST and PP, decreasing pH and salinity, and slight increases in CS. Spatial–temporal analyses revealed high present–future environmental overlay for most environmental variables. However, changes in individual environmental variables cumulatively resulted in statistically significant changes in environmental similarity. Still, the projected changes are not expected to exceed ecological thresholds, above which they would be likely to alter species' habitat suitability or to result in species distribution shifts. Anomaly analyses suggest that present–future shifts do not surpass 1/5 (pH, PP, CS) or 2/3 (salinity) of the unit, regardless of projection and area, while SST anomalies ranged from −1.1 °C to 1.1 °C. Compared to IPCC large-scale predictions for Atlantic/Mediterranean regions, the intensity of shifts on the Portuguese coast may be lower.

Keywords: Iberian coast; environmental trends; anomalies; time series; climate projections; ecosystem dynamics; habitat shifts

Academic Editor: Chin H Wu

Received: 27 April 2026
Revised: 22 May 2026
Accepted: 27 May 2026
Published: 30 May 2026

1. Introduction

Fluctuations in marine populations' abundance and presence/absence in time and space is driven by physical and biological processes. Fish production depends primarily on the fixation of carbon by net producers, which are highly impacted by environmental physical processes, and their transference along the food web [1]. The habitat of a species is determined by multiple abiotic features, and the species' response to environmental shifts is determined by how it responds to local oceanographic features. This means that species must adapt simultaneously and cumulatively to diverse environmental drivers [2]. Climate change (CC) impacts the conditions of marine habitats [3], which can influence species distribution. Therefore, understanding the impact of CC on marine habitats should

focus, a priori, on understanding future changes/trends in environmental variables and measure the degree of habitat shift related to species' optimal (present) conditions to predict species' responses.

The Portuguese coast is contained within an eastern boundary upwelling system (EBUS), which are known for their high levels of productivity and biodiversity [4]. Due to its geographic situation, the Iberian Portuguese coast is considered a transition zone with Atlantic temperate and Mediterranean and North African subtropical influences [5]. Dynamic oceanic circulation is characterized by summer wind-driven upwelling events, and during the winter, intensified river runoff feeds the Western Iberia Buoyant Plume [6], and the onset of the Iberian Poleward Current occurs [7].

Along the Portuguese coast, several shifts related to CC impacts have already been reported, including changes in water temperature and pH and shifts in wind and upwelling patterns. Between 1950 and 2010, regional warming of sea water has been reported at variable rates along the Portuguese coast [8]. An intensification of northerly winds was documented in the winter season (January and February) for the 1960–2010 period [9], while for upwelling, summer intensification has been registered for the southern coast of Portugal [10], contrasting with a slight decrease reported on the western Portuguese coast [11]. Decreasing pH levels driven by increased anthropogenic CO_2 emissions and rising SST [12,13] have been observed in the Iberian upwelling system, with coastal areas experiencing more pronounced trends [14]. Productivity is also reported to have increased in coastal areas; however, most studies assess productivity in an estuarine context [15,16].

Through its Assessment Reports, the International Panel on Climate Change (IPCC) aims to synthesize knowledge about CC and its drivers, impacts and risks and how to reduce and mitigate them. In its Sixth Assessment Report, the IPCC predicts several climate shifts for large regions in which Portugal is located, such as the north-east Atlantic and the Mediterranean basin, including: (1) a very likely decrease in precipitation in all climate projections, leading to a generally lower river runoff; (2) a likely general decrease in wind speed, resulting in lower potential wind power production; (3) an extremely likely continuation of sea level rise in the oceans surrounding Europe, ranging from +0.4 m to +0.8 m for the 2081–2100 period relative to the 1995–2014 period; and (4) a steady rise of sea surface temperatures ranging between +1 °C and +3 °C by 2100, leading to continued increases in marine heatwaves' frequency, magnitude and duration [17]. These predictions are derived from projected pathways of emissions and concentrations of greenhouse gases and aerosols and land cover and its usage [3,18], known as representative concentration pathways (RCPs). RCP projections provide a standardized approach to the assessment of potential impacts on the oceanographic environment and habitat across different geographic areas. Nevertheless, given the potential for CC-related impacts to vary across different geographical areas, it is necessary to perform regional analysis of large-scale climate change model outputs considering several RCP projections.

Due to the convergence of different ecoregions and coastal oceanographic conditions, many species with commercial economic importance are found along the Portuguese coast [19]. Climate-driven environmental changes can impact marine species in a negative or positive manner, depending on species' intrinsic characteristics [2,20]. Such impacts have the potential to trigger species' adaptive responses, including shifts in species behavior and physiology, e.g., changes in reproduction [21,22], growth [23] and mortality [24,25], as well as changes in species geographical distribution [26]. Thus, the responses of species to past and future changes in the environment can influence the structure and composition of communities [27,28] and therefore the composition, production and economic value of fishing catches [29–31].

This study aims to interpret climate multi-model projections to assess how climate change may impact environmental conditions along the Portuguese coast from a biological perspective. To achieve this, multiple analyses were applied to examine projected changes in key environmental variables. Specifically, we (i) assess annual, seasonal and monthly trends, for intermediate (RCP4.5) and business-as-usual (RCP8.5) projections, in sea surface temperature, pH, salinity, planktonic production and current strength up to the middle of the century. We also (ii) compared and quantified differences between present (2006–2020) and future (2041–2060) environmental anomalies and environmental overlay considering three oceanographic areas of the Portuguese coast; (iii) computed environmental similarity considering the differences in environmental values between present and future projections; and (iv) carried out a literature review on observed environmental shifts along the Portuguese coast. We discuss the influence of CC on environmental variables and environmental similarity and how these can impact fished species considering the range of environmental shifts between present and future scenarios found in our results.

2. Methods

2.1. Study Area

The study area matches the first slope break off the Portuguese coast and is also the most productive area of the coast [5], where most of the coastal Portuguese fishing fleet operates [32]. The Portuguese coastal region was divided into three distinct areas based on its oceanographic characteristics [5,33,34] and previous studies [10]: (1) the North area extends from the Minho River mouth at 42° N to Cabo Carvoeiro (Peniche) at 39°21′32″ N; (2), the Centre area spans from Cabo Carvoeiro to Sagres at 36°59′35″ N; and (3) the South area spans from Sagres to Vila Real de Santo António at 6° W (Figure 1).

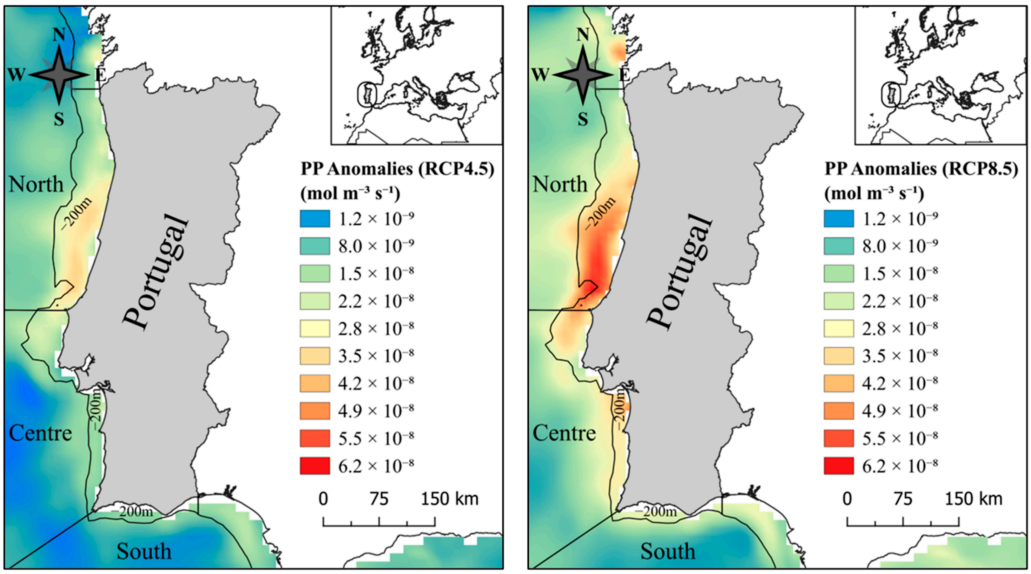

Figure 1. Portuguese coast with distinguished oceanographic areas (North, Centre and South) and 200 m bathymetric line. These maps also present the mean projected annual planktonic productivity (PP) anomaly for the 2040–2060 period, where orange and red colors indicate an increase and blue and green colors indicate a decrease in PP.

2.2. Literature Review

To understand how oceanographic environmental variables changed over past periods up to the present, a literature review of scientific studies published between 1980 and 2024 in the Portuguese coast was carried out using the Web of Science platform (http://webofknowledge.com, accessed on 27 February 2024). Using Boolean logic, specific

keywords were used (area, environmental variable name, etc.) to search for literature encompassing the selected environmental variables within the study area. For details on the methodological approach used, see Supplementary Materials S1.

2.3. Data Sources/Processing/Rationale

Marine environmental data were obtained from the Copernicus Climate Data Store. We collected data from the POLCOMS-ERSEM database (Proudman Oceanographic Laboratory Coastal Ocean Modelling System—European Regional Seas Ecosystem Model). The POLCOMS is a physical ocean circulation model that is tailored for the simulation of shelf-sea and coastal areas, while the ERSEM is an ecosystem model of marine biogeochemistry and the lower trophic levels of the marine food web [35]. The coupled POLCOMS-ERSEM system has been extensively validated against satellite and in situ observations for the Northwest European Shelf and the Mediterranean Sea, generally demonstrating a good ability to capture spatial, seasonal and temporal variability in temperature and lower trophic level dynamics [36,37]. The environmental database contains monthly 11 km gridded data for the North Atlantic for RCP4.5 and RCP8.5 projections, wherein an RCP (representative concentration pathway) uses radiative forcing (i.e., amount of energy) to calculate future projections.

From 2006 to 2060, the following monthly environmental variables were collected: sea surface temperature (SST), pH, primary productivity, secondary productivity, salinity, eastward currents (U-component) and northern currents (V-component), up to the middle of the century, for the top 20 sigma layers. Analysis of currents was restricted to the horizontal components (U and V), since vertical velocity (W) data were not available in the selected model output. Although vertical motions are important for coastal upwelling processes, the W-component is generally several orders of magnitude smaller than horizontal velocities.

To compare current climate conditions with those projected for the middle of the century, we defined two time periods: (i) present, from 2006–2020, and (ii) future (both for RCP4.5 and RCP8.5), from 2041 to 2060, following the IPCC [3]. POLCOMS-ERSEM validation by Kay et al. [36] between 2006 and 2020 demonstrated a broad agreement between observations and model outputs, allowing us to consider model projections to infer the current and future states of environmental variables. Also, we considered RCP4.5 outputs for the present given that the radiative forcing of the model between the two scenarios, between 2006 and 2020, does not differ [35]. Defining these periods allowed for comparison and measurement of differences in environmental variables between present and projected future conditions.

Monthly data were used to create different time scales: (i) an annual scale, which is the average of all months; and (ii) seasonal average scales: winter (January, February and March), spring (April, May and June), summer (July, August and September) and autumn (October, November, December).

As the spatial environmental raw data format is gridded, we calculated the monthly zonal mean, maximum and minimum environmental values by climate projection (i.e., RCP4.5 and RCP8.5) and area (North, Centre and South) up to the 200 m line.

Based on tabular data, new environmental variables were calculated: planktonic productivity (PP) and current strength (CS). PP values were obtained by summing the primary productivity and secondary productivity time series (following Bueno-Pardo et al., [2]). *CS* was calculated considering the eastward (*U*-component) and northern current (*V*-component) vectors as follows:

$$CS = \sqrt{U^2 + V^2} \quad (1)$$

2.4. Statistical Environmental Analysis

A total of 6 distinct analyses were performed; (1) exploratory analysis to assess common trends among variables and areas; (2) present–future shifts in environmental mean values and (3) environmental variables' trends, to determine whether there is an upward or downward statistical trend and its magnitude; (4) environmental overlay (EO), which consisted of evaluating the degree of interval range of environmental values between present and future; (5) anomaly analysis to assess present–future differences; and (6) environmental similarity, where all variables were considered to represent and compare the abiotic conditions between present and future. Each of these analyses is detailed below:

(1) Dynamic Factor Analysis (DFA) was used as an exploratory technique to assess annual common trends for each environmental variable (time series) across projections and areas. DFA is a multivariate time series methodology that is used to estimate underlying common patterns (trends) between non-stationary time series, i.e., attributes of the time series such as the mean, variance and autocorrelation change over time [38,39]. The DFA diagonal matrix model was used to test the relation between 6 time series (two RCP projections × three fishing areas) and 1 common DFA trend, allowing us to understand whether the different time series follow a single common trend or not. Canonical correlations were used to assess the relation between the DFA common trend and each time series, where a canonical correlation greater than 0.5 implies that the time series are statistically correlated/follows the same common trend [40].

(2) To compare present–future shifts in mean values by projection, region and time scale (annual, seasonal, monthly), the one-way ANOVA test (analysis of variance) was used. ANOVA assumptions, i.e., data normality and non-variance, were assessed with Shapiro–Wilk and Levene tests, respectively. Whenever ANOVA assumptions were not met, we employed the non-parametric alternative, the Mann–Whitney test. Present–future shifts (ANOVA/Mann–Whitney outputs) were summarized by bar-plotting the frequency of occurrence, in percentage, of significant and non-significant changes in mean values for each environmental variable.

(3) The Mann–Kendall test was used to assess trends in environmental time series (annual, seasonal and monthly) over time. This test fits a non-parametric linear regression that can be used to assess whether the overtime monotonic environmental time series represents a statistical upward or downward trend [41,42]. The slope of statistically significant trends ($p < 0.05$) was identified by the Sen's slope estimator, which calculates lines between each unique pair of points in the time series and then utilizes the median of these lines as the Sen's slope value [43]. Moreover, using median values rather than average values prevents extreme values from skewing the data [43]. The magnitude of inclination of the Sen's slope indicates the rate of variation of a given environmental variable over time [43]. To summarize the overall linear regression analysis (102 analyses per environmental variable: 12 monthly, 4 seasonal, and 1 yearly analysis for each of the three areas and across two projections), the results were bar-plotted, allowing us to understand the frequency of occurrence, in percentage, of significant and non-significant trends.

(4) The EO was estimated as the percentage of overlay between the observed and expected ranges of the different environmental variables between the present and the future periods. It was calculated using the following formula:

$$EO = \frac{P \bigcap F}{P} \times 100 \quad (2)$$

where P represents the present data range (i.e., present minimum to present maximum) for each time scale (i.e., monthly, seasonal or yearly), F represents the future data range (future minimum to future maximum) and $\bigcap$ corresponds to the intersection between

P and *F*. This index allows us to evaluate the intersection of present and future datasets (Equation (2)) and determine the percentage of values that can be found in both present and future projections, with values close to 100% meaning that present–future environmental values will match, while values close to 0% represent a null intersection of values between periods (completely dissimilar).

(5) Anomalies correspond to the difference in the mean (μ) value of environmental variables between the future and present periods (μ future − μ present). To interpret anomaly variations, anomaly classes were created to better measure the anomaly intensity range, with each observation being assigned to a specific anomaly class by variable. We used absolute values to represent anomaly variations for all the variables except for PP. Due to the unit dimension/scale of PP (E^{-08} mol m^{-3} s^{-1}), we presented it in percentage classes (e.g., 0–10% etc.). This decision was related to the difficulty in interpreting present–future value shifts when we are dealing with 7 to 8 decimal places in exponential values. Histograms were plotted, with different ranges of size–class anomalies, to better understand anomaly distribution in each variable.

(6) Given that shifts in abiotic conditions constrain species habitat selection/suitability [27], we evaluated environmental similarity as the joint effect of the different environmental variables by estimating similarity differences between present–future projections, following the Hutchinsonian niche concept and established practices in Species Distribution Modelling (SDMs/ENMs), where environmental variables at species occurrence locations are used as proxies for the species' fundamental niche in environmental space [44–46]. Since all variables are expressed in different units, a minimum–maximum normalization (i.e., 0 to 1 normalization) was performed for each environmental variable, removing the effect of variable unit weight before calculating differences (changes) in habitat. A similarity matrix based on Euclidean distance was built for each variable for each projection (RCP4.5 and RCP8.5), region (North, Centre, South) and time scale (month, season and year). Euclidean distance was chosen since it is the standard metric used in multivariate environmental analyses in normalized environmental space [47]. Then, habitat differences between present and future projections were assessed by conducting an analysis of similarity (ANOSIM) between the present (2006–2020) and future (2041–2060) for each projection, area and time scale, resulting in a total of 102 analyses. Whenever statistical differences were observed, the SIMPER (similarity percentages) test was used to identify the environmental variables that explained most present–future differences [48]. Euclidian distance output does not provide direct similarity, and it was subsequently transformed into a similarity percentage as follows: $\text{Similarity}\ (\%) = \left(1 - d/\sqrt{x}\right) \times 100$, where d represents the Euclidean distance between two min–max normalized observations and x the number of variables. Division by $\sqrt{x}$ (the theoretical maximum Euclidean distance when all variables are normalized between 0 and 1) implies the similarity index is bound between 0 and 100%. Similarity values between time periods close to 100% indicate little to no environmental similarity, while values close to 0% similarity (or 100% dissimilarity) indicate a great degree of environmental shift between present and future.

3. Results

3.1. Literature Review

Most studies on time series did not present results by area but rather for the whole Portuguese coast. The result of the first search yielded a total of 50 articles. We excluded 36 (lacking time series or trend data/analyses) and kept 14 articles for the current analysis/discussion. The literature review (see Supplementary Materials S1—Table S1) revealed that, for the Portuguese coast, SST (n = 6) was the most studied variable, followed by PP (n = 4, including primary and secondary production studies). Conversely, time series analyses focusing on salinity, pH and CS were less frequent. The six studies on SST in-

dicated a general temperature increase, while trends in other environmental variables showed wide variability and, in general, few statistically significant trends (Supplementary Materials S1—Table S1).

3.2. Environmental Variable Analysis

The DFA with the lowest Akaike information criterion conducted for the SST time series identified a single common trend that increases over time (Supplementary Materials S1—Figure S1). However, the only regional trend statistically correlated (i.e., canonical correlation > 0.5) with the general DFA common trend occurred in the South area for RCP8.5. The remaining canonical correlations are weak (<0.5). The PP DFA common trend suggests an overall increase in PP regardless of area or projection, with a peak around the year 2045 followed by a slight decrease over the following decade. For CS, the DFA common trend presented an increasing trend, and all time series were positively correlated with the DFA common trend. Detailed DFA outputs are available in Supplementary Materials S1—Figures S1–S3.

A clear shift between present and future can be observed for salinity and pH (Figure 2). In contrast, for SST, PP and CS, shifts are not as noticeable, evidencing a lower degree of change in mean values (Figure 2). Detailed information about mean and minimum–maximum (min–max) values by projection and area, for each environmental variable, is provided in Supplementary Materials S1; Tables S7–S11.

Statistical shifts in present–future mean values were detected for SST (ANOVA/Mann–Whitney tests, n = 102 analyses for each variable) in 22% of analyses (Figure 3A). For pH, salinity, PP and CS, statistically significant differences in present–future mean values were recorded for 96, 100, 70 and 62% of the analyses (Figure 3A).

Regarding the analysis of trends in environmental variables, statistically significant increasing trends were detected for SST, CS and PP in 25, 35 and 50% of regression analyses. Decreasing trends represented 4% of the analyses in SST, while for CS and PP, no decreasing trends were statistically significant (Figure 3B). For pH and salinity, 90 and 100% of the trends showed statistically significant decreasing trends (Figure 3B).

Statistically significant shift rates varied between a minimum–maximum (min–max) of –0.26 (June, RCP4.5, North) and 0.24 °C (September and December, RCP8.5, South) per decade for SST; there was a maximum decline around −0.04 (May, RCP4.5, North) for pH (no increase trend in any pH analyses); a min–max of −0.17 PSU (March and April, RCP8.5, North) and −0.02 PSU (multiple analysis) for salinity; min–max values of 5.20×10^{-10} (winter, RCP4.5, South) and 5.46×10^{-8} (July, RCP4.5, North) for PP; and a maximum of 0.01 m s^{-1} (several months/projections) for CS. Detailed statistical outputs and plots are available in Supplementary Materials S1 (Tables S12–S26).

The general environmental overlay (EO) analyses (Figure 4) revealed that the overlay between present–future datasets varied between 68 (autumn, RCP8.5, South area) and 100% (multiple combinations; n = 39 out of 102), with a mean around 95%, for SST; 46 (July, RCP4.5, Centre area) to 100 (several combinations; n = 14 out of 102), with a mean around 87%, for pH; 38 (March, RCP8.5, South) to 91% (annual, RCP4.5, Centre area), with a mean around 75%, for salinity; 53 (August, RCP8.5, Centre area) to 100% (several combinations; n = 26 out of 102), with a mean around 92%, for PP; and 53 (April, RCP8.5, South area) to 100% (several combinations; n = 39 out of 102), with a mean around 93%, for CS. See Supplementary Materials S1, Figure S5 for full details.

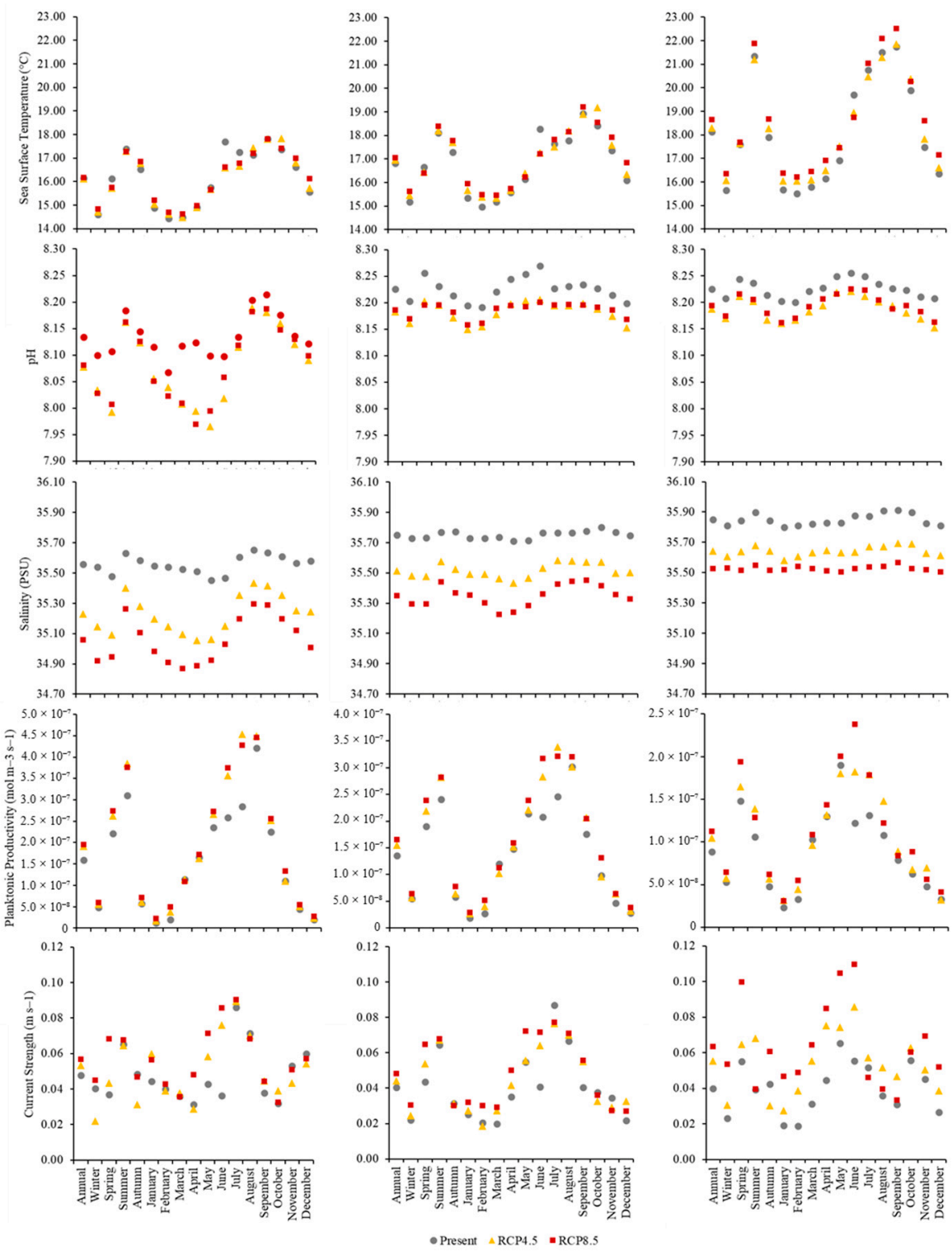

Figure 2. Mean environmental values for each variable for each projection (RCP4.5 and RCP8.5), area (North, Centre, South) and time scale (year, season, month). Information about statistical changes in mean values between present–future projections are provided in Figure 3A.

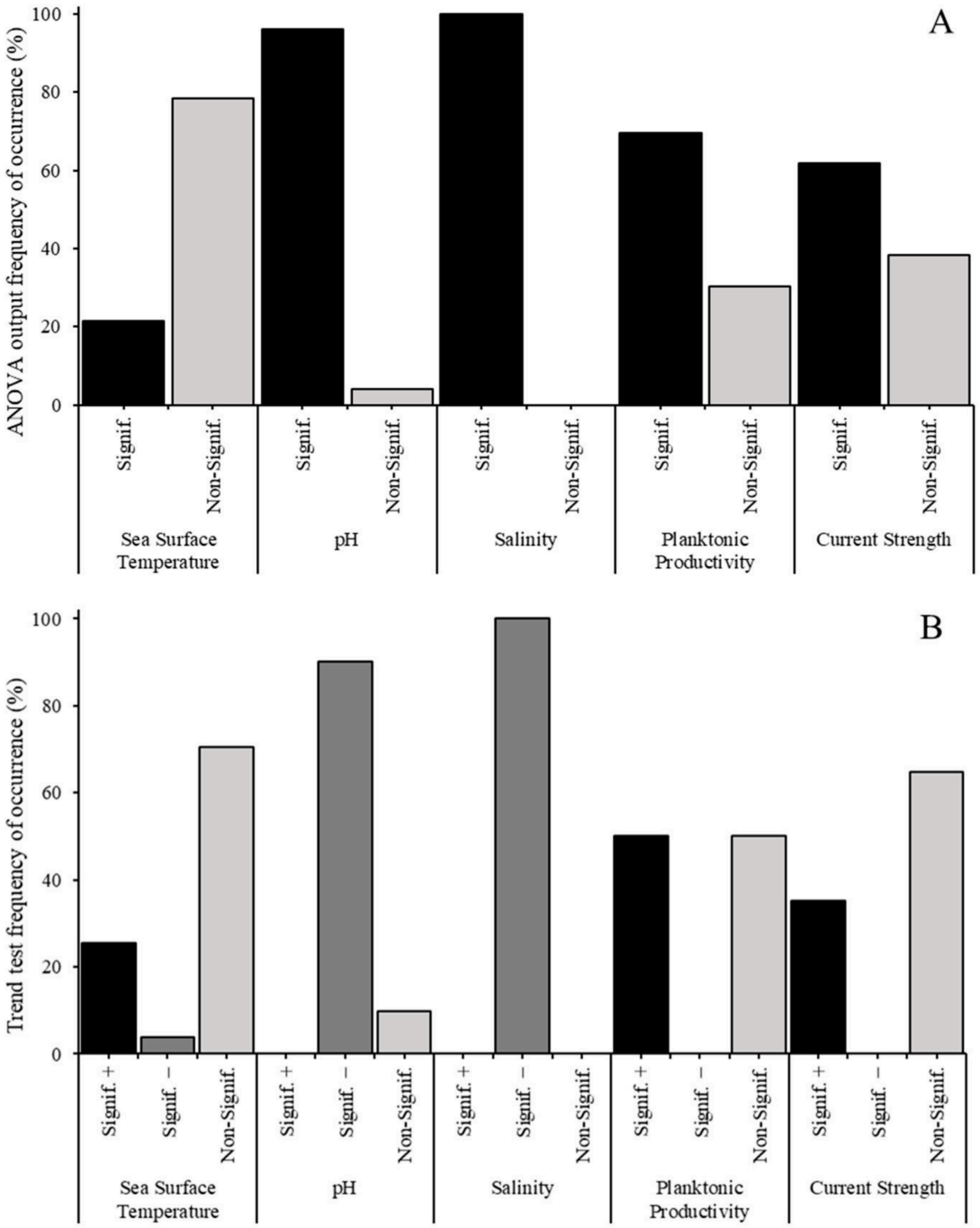

Figure 3. (**A**) Frequency of occurrence, in percentage, of ANOVA/Mann–Whitney-identified statistical changes (significant and non-significant differences between present–future mean values) conducted for mean, annual, seasonal and monthly environmental data, considering both projections by area. Information regarding individual analyses is available in Supplementary Materials S2. (**B**) Summary of overall regression analysis results (102 per environmental variable, corresponding to yearly, seasonal and monthly analyses per region and projection) with the frequency of occurrence of trend results. Increase (plus sign) and decrease rates (minus sign) are highlighted by the b-slope of the regression analyses. Information regarding individual regression analyses can be found in Supplementary Materials S1—Figures S6–S20 and Tables S12–S26.

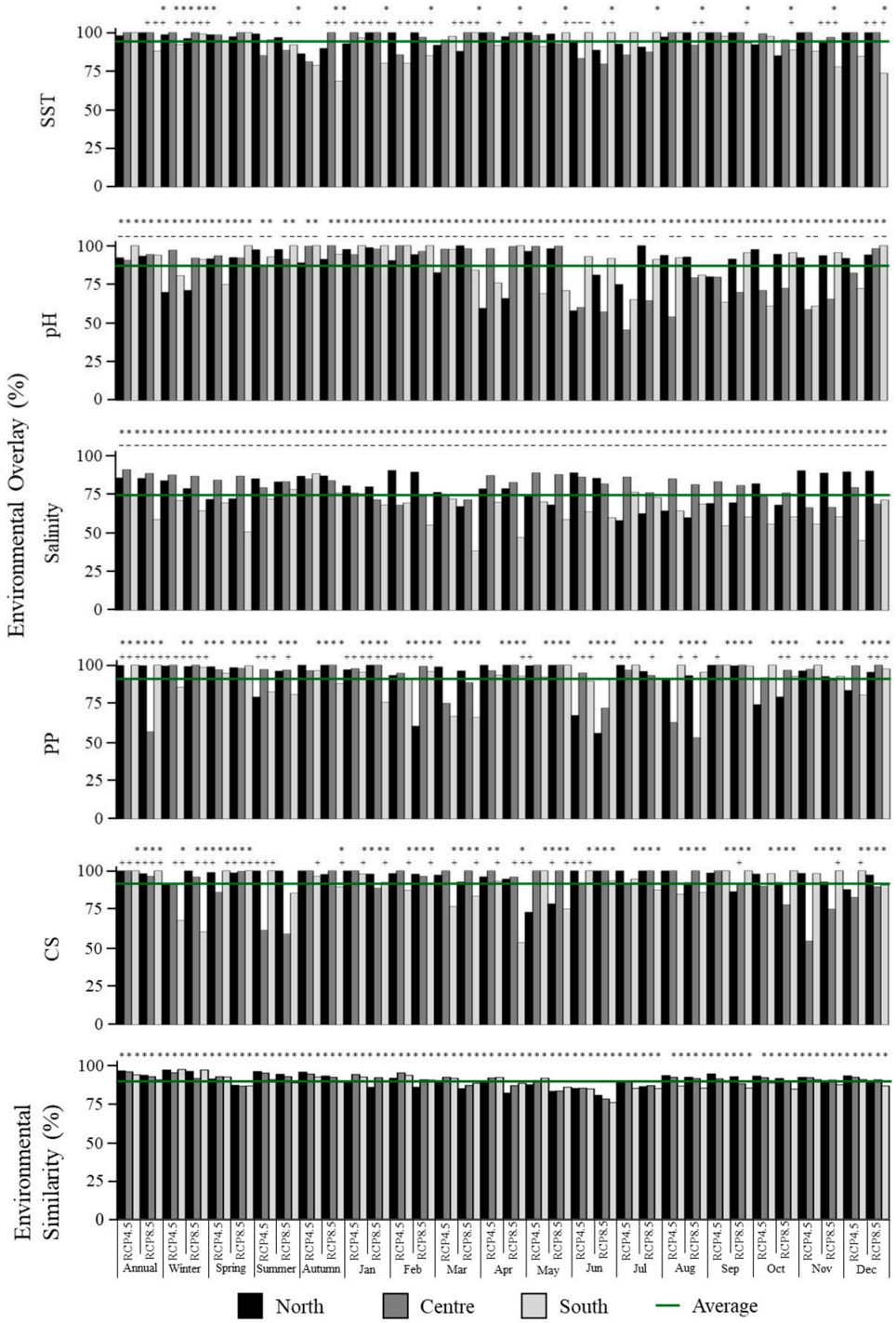

Figure 4. Environmental overlay (EO), in percentage of overlay, between present and future projections, showing the range of values for each environmental variable by area, time scale (annual, seasonal and monthly) and projection (RCP4.5 and RCP8.5), with a total of 102 analyses per environmental variable. Environmental similarity represents shifts resulting from the contribution of changes in all environmental variables, displayed as differences between the present and future projections. The horizontal line represents the mean EO or similarity value for all analyses. Significant differences between present and future, identified using ANOVA/Mann–Whitney tests, are indicated by an asterisk (*). Significant trends identified using the Mann–Kendall test are shown using a plus sign (+) for positive trends and a minus sign (−) for negative trends. Detailed information on EO for each individual analysis (i.e., projection, region and time scale) is provided in Supplementary Materials S1.

Regardless of RCP projection, the most common present–future EO ranges were between 80 and 100%. The EO frequency of occurrence was 85, 72, 86 and 89% for SST, pH, PP and CS, respectively. Salinity displayed a different pattern regarding EO (%), with three EO classes (50–60; 60–70; 70–80%) comprising 61% of the EO for all analyses performed, with the 80 to 100% class comprising 37% of the analyses (Figure 5).

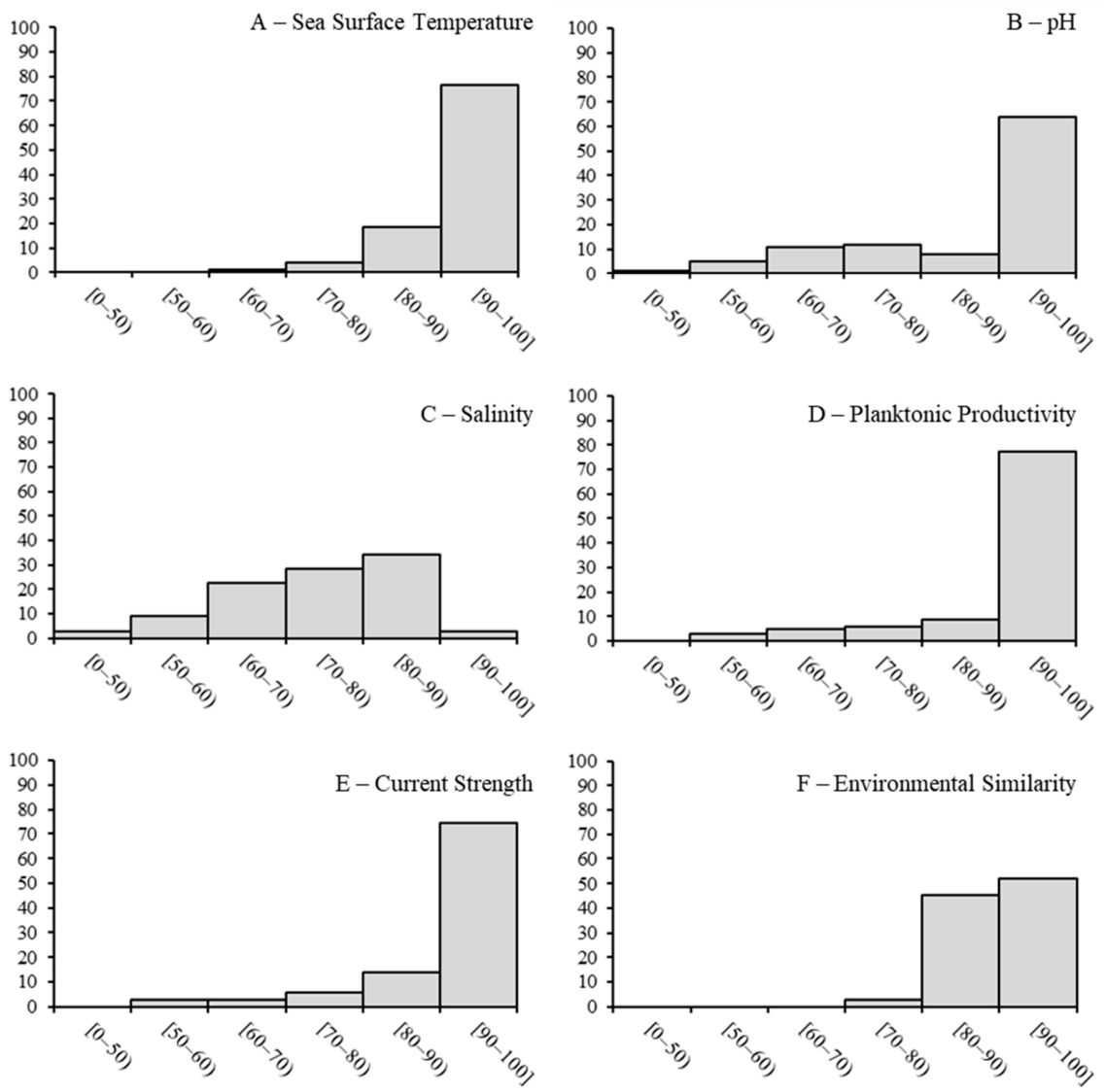

Figure 5. Histogram plots showing the frequency of occurrence of EO (environmental overlay) class distribution (in percentage) for each environmental variable ((**A**–**E**) plots) and environmental similarity (plot (**F**)) between present and future, regardless of area (North, Centre, South) or time scale (annual, seasonal and monthly). Each plot contains a total of 102 analysis for each environmental variable.

Anomaly histogram analyses (Figure 6) revealed that the frequency of occurrence of anomaly classes representing half of the unit of the environmental variable (anomalies not reaching half of the unit), up to the middle of the century, is high. Anomalies range from –0.4 to +0.4 °C in 64% of SST analyses; 0 to –0.15 in 100% of pH analyses; –0.1 to –0.5 PSU in 91% of salinity analyses; and –0.01 to 0.06 m s^{-1} in 100% of CS analyses. Regarding PP anomaly results, the most frequent anomaly classes ranged from 0 to 60% and occurred in 84% of the analysis, indicating a general increase in PP.

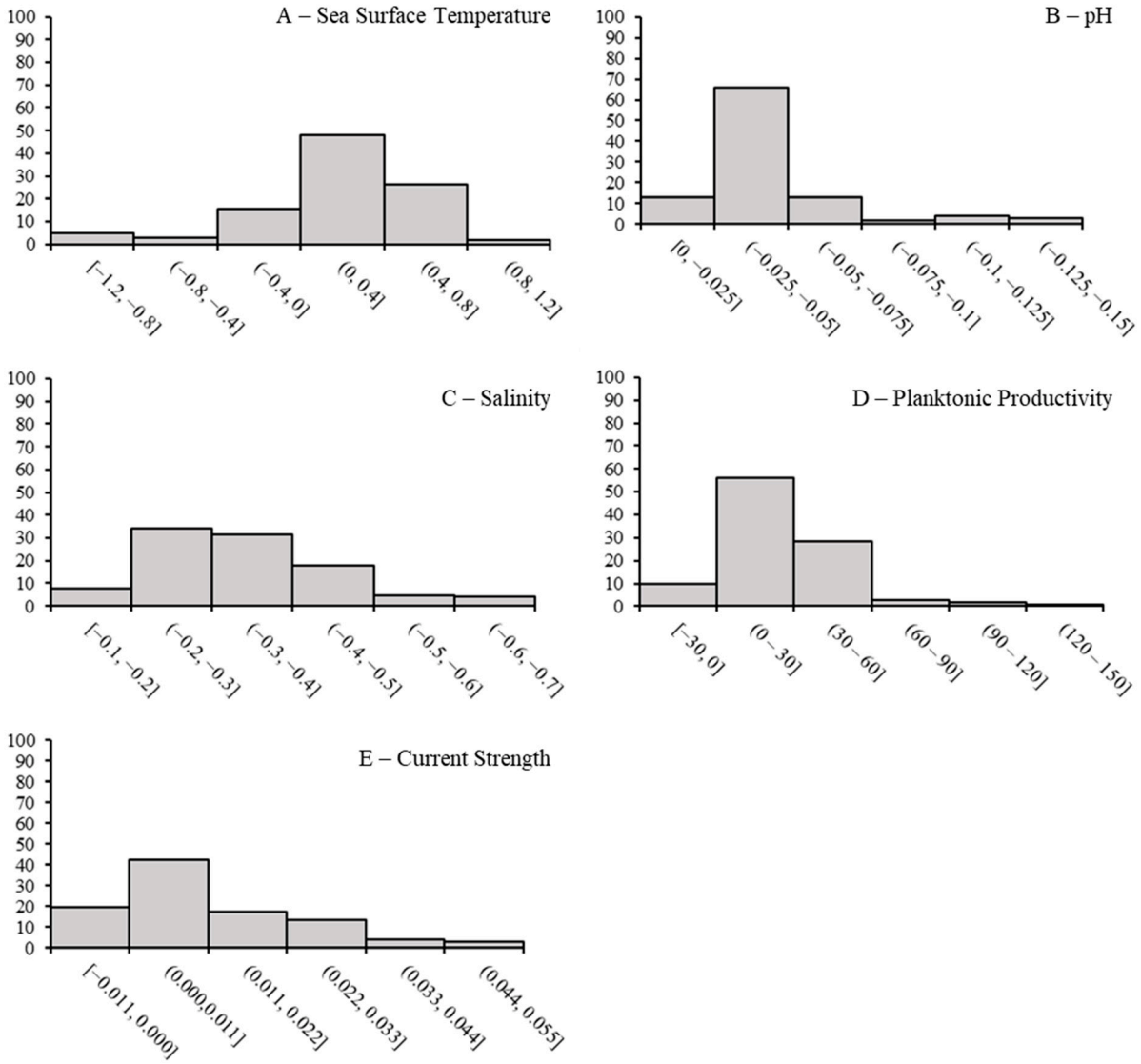

Figure 6. Environmental variable anomaly histogram plot showing frequency of occurrence (in percentage) by anomaly class, regardless of the projection, area or time scale (annual, seasonal and monthly).

SST anomalies between −1.2 and −0.4 °C (higher anomaly classes indicating SST decrease) and 0.4 to 1.2 (higher anomaly classes indicating SST increase) recorded a frequency of occurrence of 8 and 28%. For salinity, the –0.5 to –0.7 PSU anomaly classes (higher anomaly classes indicating salinity decrease) recorded a frequency of occurrence of 9%. For PP, only 10% of the analysis revealed negative anomalies (Figure 6).

Annual SST anomalies ranged from −0.02 °C (RCP4.5, North) to 0.52 °C (RCP8.5, South), seasonal anomalies ranged from −0.39 °C (spring, RCP4.5, North) to 0.68 °C (winter, RCP8.5, South) and monthly anomalies ranged from −1.10 °C (June, RCP4.5, North) to 1.10 °C (November, RCP8.5, South). Annual pH anomalies ranged from −0.06 (RCP4.5, North) to −0.03 (RCP8.5, North), seasonal anomalies ranged from –0.11 (spring, RCP4.5, North) to −0.03 (spring, RCP8.5, South) and monthly anomalies ranged from −0.15 (April, RCP8.5, North) to −0.01 (November, RCP8.5, North). Annual salinity anomalies ranged from –0.50 PSU (RCP8.5, North) to –0.21 PSU (RCP4.5, South), seasonal anomalies ranged from –0.6 PSU (winter, RCP8.5, North) to –0.19 PSU (winter, RCP8.5, South) and monthly anomalies ranged from –0.66 PSU (March, RCP8.5, North) to –0.18 PSU (July, RCP4.5, Centre). Annual PP anomalies (in %) ranged from 14% (RCP4.5, South) to 27% (RCP8.5,

North), seasonal anomalies ranged from 3% (winter, RCP4.5, Centre) to 34% (summer, RCP4.5, North) and monthly anomalies ranged from −14% (March, RCP4.5, Centre) to 150% (July, RCP4.5, North). Annual CS anomalies ranged from 0.004 m s^{-1} (RCP4.5, Centre) to 0.023 m s^{-1} (RCP8.5, South), seasonal anomalies ranged from −0.003 m s^{-1} (autumn, RCP8.5, South) to 0.045 m s^{-1} (spring, RCP8.5, South) and monthly anomalies ranged from –0.010 m s^{-1} (July, RCP4.5, Centre) to 0.054 m s^{-1} (June, RCP8.5, South). Full details regarding anomaly analysis are available in Supplementary Materials S1—Figure S21.

Environmental change results (Figure 5, panel F), provided by the individual contributions of all environmental variables, evidenced statistically significant changes between all present–future projection analyses performed, except for the months of August and October in the RCP4.5 projection in the North area (detailed ANOSIM results are available in Supplementary Materials S1, Tables S27–S29). The overall average similarity varied between 45.29% (June, RCP8.5, South) and 92.67% (February, RCP8.5, Centre area) with a mean similarity of around 76.3%. Environmental similarity classes between 70 and 80 (34% of the analyses) and between 80 and 90 (37% of the analyses) comprised 71% of the analyses made (Supplementary Information S1—Figure S5). Salinity followed by pH comprised the variables that generally contributed the most towards differences between present and future (Supplementary Materials S1; Table S30), while PP followed by SST comprised the variables that generally contributed the least to differences between present and future (Supplementary Materials S1; Table S31).

4. Discussion

The projected changes presented in this study should be interpreted in light of the uncertainties that are inherent to climate model projections. The Copernicus marine products used here provide scenario-based projections under RCP4.5 and RCP8.5, generated using coupled physical–biogeochemical modelling. As with similar climate projection datasets, uncertainty can arise from several sources, including the choice of emissions pathway, the driving global and regional climate models, the ocean and biogeochemical model structure, model parameterization, boundary conditions and natural climate variability. Thus, greater confidence can generally be placed in future changes expected to show a similar direction under both RCP4.5 and RCP8.5, particularly when they occur over broader spatial scales or longer time periods. Conversely, more caution is needed when interpreting local-scale patterns, coastal or shallow-water areas, and variables that may be more sensitive to biogeochemical parameterization or boundary inputs. These uncertainties do not prevent the use of the projections for assessing possible climate-driven changes, but they should be considered when evaluating the magnitude and local consequences of the projected response.

Differences between present and future environmental conditions for RCP4.5 and RCP8.5 projections were assessed for three regions of the Portuguese coast (0 to 200 m bathymetry). Overall, future environmental trends include increases in SST and PP and decreases in pH and salinity, while CS changes are expected to be minimal. The overlay between present and future environmental ranges for the different variables was generally high, indicating that future conditions would largely be within the range of present conditions, at least until the middle of the century. In addition, anomaly analyses revealed that, up to the middle of the century, estimated present–future shifts do not surpass $\frac{1}{5}$ (pH; PP, CS) or $\frac{2}{3}$ (salinity) of the unit regardless of projection or area. These findings may not be surprising given the location of the Portuguese continental coast within the Canary eastern boundary upwelling system (EBUS) and its intermediate latitudinal range, which favours wide environmental variability [11]. However, it should be noted that habitat changes derived from the cumulative effects of all environmental variables revealed statistically

significant present–future changes, regardless of area or projection. These changes are discussed below.

The IPCC projects sea surface temperature (SST) increases across Europe of +1 °C to +3 °C by 2100 [3], implying warming rates of approximately +0.125 °C to +0.375 °C per decade. Along the Portuguese coast, however, present results point to slower warming trends, ranging from +0.09 °C (Centre) to +0.15 °C (South) per decade. These values are consistent with previous studies reporting an average warming rate of approximately +0.15 °C per decade [8,49–51]. This comparatively slower warming has been linked to regional oceanographic processes, particularly coastal upwelling. Upwelling events can significantly buffer long-term SST increases in shelf and slope waters [52] and may even be related to the seasonal cooling observed in June (see Supplementary Materials S1, Figure S1). According to the Bakun hypothesis [53], climate-driven intensification of land–sea thermal gradients may strengthen alongshore winds, promoting intensified coastal upwelling in eastern boundary current systems. Along the western Iberian coast, northerly winds are the primary drivers of coastal upwelling and promote offshore Ekman transport and the upwelling of colder subsurface waters [50], buffering regional sea surface warming trends relative to large-scale IPCC projections. However, upwelling intensity within the Iberian EBUS remains spatially and temporally variable and may also be modulated by large-scale atmospheric patterns such as the North Atlantic Oscillation (NAO), which can influence regional warming patterns along the Portuguese coast [54,55]. Similar thermal buffering effects associated with coastal upwelling have also been reported in the California, Humboldt and Benguela systems, although their magnitude and persistence vary regionally [56,57]. Nevertheless, reduced warming rates do not imply an absence of ecological risk or vulnerability. Many marine species, particularly during more sensitive development stages, may still be negatively impacted by what may be perceived as relatively small temperature anomalies or environmental shifts. Thus, although slower warming may delay surpassing species' thermal tolerance thresholds, continued environmental change may still influence species' phenology and distribution over longer timescales [22,58,59]. Indeed, as SST rises beyond species' thermal tolerance limits, marine organisms may shift their geographical distributions to remain within optimal temperature ranges [60]. Consistent with this expectation, recent studies have documented the emergence of subtropical species along the southern Portuguese coast [59,61,62], with evidence of poleward expansion. Based on the SST trends identified in the present study, this warming trajectory is expected to persist at least until the mid-21st century.

Ocean warming and ocean acidification are concurrent consequences of anthropogenic climate change. Although increasing seawater temperature reduces CO_2 solubility, the continued rise in atmospheric CO_2 concentrations drives ocean CO_2 uptake, leading to decreases in seawater pH through carbonate system reactions [63]. For the North Atlantic, the IPCC reported a very likely decrease in oceanic pH, ranging from −0.1 to −0.2, for the period between 2041 and 2060 relative to the 1981–2010 baseline under the RCP8.5 projection [64]. According to the IPCC, surface ocean pH is very likely to have decreased since the 1980s at a rate of −0.016 to −0.020 per decade in the subtropics, and at a rate of –0.002 to −0.026 per decade in the subpolar and polar regions [3,65]. In the present study, declining pH trends at the annual scale do not surpass −0.01, which is below the results detailed by Gutiérrez et al. [64], although comparison baselines do differ between studies (i.e., 1981–2010 for Gutiérrez et al. [64] and 2006–2020 for the present study). Nevertheless, current trends are in line with or occurring at a lower rate of change than those reported by the IPCC (see Supplementary Materials S1, Figure S5) [3,65,66]. UK fishery studies within the 2020–2050 timeframe suggest that acidification resulting from SST increases (ranging from +0.5 to +3.3 °C, with the consequent pH decrease ranging from

−0.04 to −0.37) would imply revenue losses ranging from 1 to 21%, wherein fisheries targeting bivalves would be on the forefront of revenue loss comparing to other fisheries, e.g., bonefish or cephalopods [67]. Comparatively, in Portuguese fisheries, CC has been linked to shifts in landing trends [58,61] and lower revenues for sardine (*Sardina pilchardus*) fisheries [68]. The distribution ranges of many of the commercial species found the UK also cover Portugal. Therefore, it can be hypothesized that Portuguese fisheries (e.g., bivalves) may face similar challenges to those identified by Fernandes et al. [67]. In Portugal, the maximum decadal SST increase and pH decrease were 0.33 °C (September) and −0.04 (May), respectively, meaning that maximum trends are recorded in specific months and do not prevail throughout the year/season. For the next three decades, on the Portuguese coast, SST can rise by 1 °C in September and pH can drop by −0.1, both of which are values globally lower than those recorded by Fernandes et al. [67] in the UK. The joint effect of rising SST along with the increasing CO_2 absorption rates, i.e., decreasing oceanic pH, are likely connected to the generalized increasing anomalies in coastal PP [1]. However, relations between PP and SST are not always direct. In open ocean, chlorophyll-a, an important component of primary production, tends to decrease when SST increases [69], which can help in explaining decreasing PP anomalies offshore (Figure 1). A general increase in coastal PP is expected in the future, although PP environmental overlay remains high in most circumstances (92% average).

Among all the environmental variables, the lowest average EO (~74%) was registered for salinity, with all trends denoting decreases, particularly for RCP8.5 in the North. According to the IPCC's fifth assessment report, changes in salinity in the last 50 years were basin-dependent, with increases in evaporative regions and decreases in regions where rainfall is predominant, according to chapter 3.3 in [70]. A reconstruction study of global salinity changes since 1960 [71] also points to basin-dependent shifts, with increases in the Atlantic Ocean, but with the global freshening of oceans (i.e., decreasing salinity) ranging from 1.9 to 5.2%. Overall, the results evidenced decreasing salinity near the shore (see Figures 2, 3A,B, 4, 5C and 6C), as present–future min–max salinity anomalies ranged between –0.66 and –0.18 PSU in specific months. This means that min–max anomalies are varying between decreases of 1.85% and 1%, which are values below those reported by Cheng et al. [71]. Such differences may be related to the location of Portugal within the transition zone between evaporation-dominant (to the south) and precipitation-dominant (to the north) Atlantic areas ([70] Rhein et al., 2013). In the Atlantic, the reasons behind shifts in salinity remain uncertain and are often linked to deglaciation processes or shifts in the Atlantic Multidecadal Oscillation and North Atlantic Oscillation, as well as shifting rainfall patterns [70,71]. However, local changes in nearshore salinity on the Portuguese coast in specific months or seasons likely result from shifts in river runoff. That is the case in the north of Portugal, where the Western Iberian Buoyant Plume (WIBP), a surface, low-salinity water lens formed by river discharge [52], occurs in the winter. For small–medium pelagic species, the combination of winter upwelling with retention mechanisms such as the WIBP, which coincides with the spawning peak of these species, leads to increased chances of larval survival on the Portuguese coast [72–74]. Therefore, the results evidence that, in the North, where salinity decreases are expected to be more pronounced, predominantly during the winter and spring, the favorable conditions for species recruitment are expected to be maintained.

CS was the environmental variable with less anomaly changes and lower decadal shift rates. The anomaly intensity (anomaly classes) was found to be very low, with the maximum anomaly class (0.044–0.055 m s^{-1}) comprising around 1/20 of the CS unit, and with average EO around 93%. Changes in CS were also more evident in the South area, where a general intensification of currents is expected. This result can be associated with

the intensification of westerly winds on the southern Portuguese coast [75]. Seasonally stable current regimes are important to disseminate and/or trap larvae near nurseries [76], increasing survivorship during pre-flexion stages, when fish larvae have limited swimming capabilities [77]. Indeed, swimming capacity plays an important role during recruitment, favoring larvae that follow chemical clues and are also transported by the currents [78,79]. In this regard, sedentary fish are expected to be more sensitive to habitat shifts than changes in currents, while highly mobile fish are expected to be more sensitive to changes in currents than habitat shifts [27]. Results support the suggestion that present CS conditions will not change to levels that can disrupt eggs and/or larvae dispersion thresholds during the early life stages of marine species along the Portuguese continental shelf by the middle of the century.

The EO analysis evidenced a high level of overlap between present and future conditions ranging between 80 and 100%, for most environmental variables in most individual analyses made. However, the habitat approach revealed statistically significant habitat changes in almost all analyses made. This indicates that changes among all environmental variables cumulatively lead to potential habitat changes that cannot be foreseen when looking at a single variable at a time. Still, these results should be contextualized regarding the likely impact on species at an ecological level, namely if such statistical habitat changes are expected to surpass a physical environment threshold that constrains the species' range of occurrence in the future. In fact, we found that the frequency of the highest and lowest class ranges—i.e., the "tail classes"—of anomaly distribution had a very low percentage of occurrence in the future. Furthermore, in most cases, the highest class range of each environmental variable does not surpass one quarter (pH, PP, CS) or one half (SST, salinity) of a unit shift for the middle of the century. All in all, habitat changes were mostly explained by pH in the RCP4.5 and salinity in the RCP8.5, which are also the two environmental variables with the lowest EO percentages. This finding is most likely related to salinity and pH being overall more stable environmental variables year-round, regardless of time scale or area, and thus, any changes to these values are easily detectable by the EO method. Moreover, regression analyses for SST, PP and CS displayed many non-significant trends; that is, linear increase over time is not expected in many space–time combinations.

Results pertaining to habitat changes lead to questions about the timing of environmental changes, as most anomalies and rate shifts were found to occur at different spatial–temporal combinations. Hypothetically, if min–max (i.e., anomaly tail classes) environmental shifts would occur synchronically at a particular space–time combination, and if these trends were to persist through the year/season/month for a given variable, then we would expect higher habitat shifts from present conditions. However, large anomaly/trend changes in environmental conditions are not perceived to be synchronic. Although statistical habitat changes were registered, at an individual environmental variable level, future value ranges slightly differed from present conditions. Based solely on the range of environmental variables, most species' habitat thresholds are not likely to be exceeded; however, additive or synergistic effects (e.g., warming and acidification together) could still affect sensitive life stages.

5. Conclusions

The combination of multiple analyses allowed us to unravel the potential impacts of climate change on the Portuguese marine environment, considering two climate change scenarios. Projected changes included increasing SST and PP, slight increases in CS and decreasing pH and salinity. These patterns were consistent across analyses (i.e., DFA and Mann–Kendall trend tests), suggesting a high likelihood of continued environmental change over time. However, tail-end anomaly distributions (i.e., the most extreme anoma-

lies) exhibited very low probabilities of occurrence and were generally not synchronous across variables, contributing to lower overall environmental change. Warming trends were more pronounced in southern Portugal and during the winter months relative to other regions and seasons. Additionally, the EO index enabled direct comparison among environmental variables by standardizing their relative magnitude of change under projected climate conditions, revealing generally high overlap between present and future environmental conditions.

Overall, projected environmental changes along the Portuguese coast appear to be less pronounced than those reported for large-scale IPCC regions. This pattern is likely associated with the location of the Portuguese coast within an EBUS, where coastal upwelling may partially buffer regional climate-driven oceanographic changes. Nevertheless, even relatively small but persistent environmental shifts may have important ecological consequences, particularly during sensitive stages of species life cycles.

Supplementary Materials: The following supporting information can be downloaded at: https://www.mdpi.com/article/10.3390/w18111326/s1.

Author Contributions: Conceptualization, M.M.-A. and F.L.; methodology, M.P., J.B.-P., M.M.-A. and F.L.; software, M.P. and J.B.-P.; validation, J.B.-P., M.M.-A. and F.L.; formal analysis, M.P.; investigation, M.P.; resources, J.B.-P., M.M.-A. and F.L.; data curation, M.P.; writing—original draft preparation, M.P.; writing—review and editing, J.B.-P., M.M.-A. and F.L.; visualization, J.B.-P., M.M.-A. and F.L.; supervision, J.B.-P. and F.L.; project administration, F.L.; funding acquisition, M.P., J.B.-P. and F.L. All authors have read and agreed to the published version of the manuscript.

Funding: This study received Portuguese national funds from FCT-Foundation for Science and Technology through contracts UID/04326/2025 (https://doi.org/10.54499/UID/04326/2025), UID/PRR/04326/2025 (https://doi.org/10.54499/UID/PRR/04326/2025) and LA/P/0101/2020 (DOI:10.54499/LA/P/0101/2020). FL was supported by FCT: DL57/2016/CP1361/CT0008 and 2022.04803.CEECIND. MP was funded by FCT PhD fellowship SFRH/BD/11426/2022, https://doi.org/10.54499/2022.11426.BD. JBP was supported by EU Horizon 2020 HORIZON-CL6-2021-BIODIV-01-04 agreement No 101060072 "ACTNOW".

Data Availability Statement: The original data presented in the study are openly available through the Copernicus Climate Data Store at https://cds.climate.copernicus.eu/datasets/sis-marine-properties?tab=overview or at https://doi.org/10.24381/cds.dcc9295c (accessed on 1 June 2020).

Conflicts of Interest: The authors declare no conflicts of interest.

References

1. Dutkiewicz, S.; Morris, J.J.; Follows, M.J.; Scott, J.; Levitan, O.; Dyhrman, S.T.; Berman-Frank, I. Impact of Ocean Acidification on the Structure of Future Phytoplankton Communities. *Nat. Clim. Change* **2015**, *5*, 1002–1006. [CrossRef]
2. Bueno-Pardo, J.; Nobre, D.; Monteiro, J.N.; Sousa, P.M.; Costa, E.F.S.; Baptista, V.; Ovelheiro, A.; Vieira, V.M.N.C.S.; Chícharo, L.; Gaspar, M.; et al. Climate Change Vulnerability Assessment of the Main Marine Commercial Fish and Invertebrates of Portugal. *Sci. Rep.* **2021**, *11*, 2958. [CrossRef]
3. IPCC. *Climate Change 2021: The Physical Science Basis. Contribution of Working Group I to the Sixth Assessment Report of the Intergovernmental Panel on Climate Change*; Masson-Delmotte, V., Zhai, P., Pirani, A., Connors, S.L., Péan, C., Berger, S., Caud, N., Chen, Y., Goldfarb, L., Gomis, M.I., et al., Eds.; Cambridge University Press: Cambridge, UK; New York, NY, USA, 2021; 2391p. [CrossRef]
4. García-Reyes, M.; Sydeman, W.J.; Schoeman, D.S.; Rykaczewski, R.R.; Black, B.A.; Smit, A.J.; Bograd, S.J. Under Pressure: Climate Change, Upwelling, and Eastern Boundary Upwelling Ecosystems. *Front. Mar. Sci.* **2015**, *2*, 109. [CrossRef]
5. Bettencourt, A.M.; Bricker, S.B.; Ferreira, J.G.; Franco, A.; Marques, J.C.; Melo, J.J.; Nobre, A.; Ramos, L.; Reis, C.S.; Salas, F.; et al. *Typology and Reference Conditions for Portuguese Transitional and Coastal Waters*; Institute of Marine Research: Lisbon, Portugal, 2004.
6. Otero, P.; Ruiz-Villarreal, M.; Peliz, A. Variability of River Plumes off Northwest Iberia in Response to Wind Events. *J. Mar. Syst.* **2008**, *72*, 238–255. [CrossRef]

7. Peliz, Á.; Dubert, J.; Santos, A.M.P.; Oliveira, P.B.; Le Cann, B. Winter Upper Ocean Circulation in the Western Iberian Basin—Fronts, Eddies and Poleward Flows: An Overview. *Deep Sea Res. Part I Oceanogr. Res. Pap.* **2005**, *52*, 621–646. [CrossRef]
8. Baptista, V.; Silva, P.L.; Relvas, P.; Teodósio, M.A.; Leitão, F. Sea Surface Temperature Variability along the Portuguese Coast since 1950. *Int. J. Climatol.* **2018**, *38*, 1145–1160. [CrossRef]
9. Leitão, F.; Relvas, P.; Cánovas, F.; Baptista, V.; Teodósio, A. Northerly Wind Trends along the Portuguese Marine Coast since 1950. *Theor. Appl. Clim.* **2019**, *137*, 1–19. [CrossRef]
10. Leitão, F.; Baptista, V.; Vieira, V.; Laginha Silva, P.; Relvas, P.; Alexandra Teodósio, M. A 60-Year Time Series Analyses of the Upwelling along the Portuguese Coast. *Water* **2019**, *11*, 1285. [CrossRef]
11. Barton, E.D.; Field, D.B.; Roy, C. Canary Current Upwelling: More or Less? *Prog. Oceanogr.* **2013**, *116*, 167–178. [CrossRef]
12. Caldeira, K.; Wickett, M.E. Anthropogenic Carbon and Ocean pH. *Nature* **2003**, *425*, 365. [CrossRef] [PubMed]
13. Doney, S.C.; Fabry, V.J.; Feely, R.A.; Kleypas, J.A. Ocean Acidification: The Other CO_2 Problem. *Annu. Rev. Mar. Sci.* **2009**, *1*, 169–192. [CrossRef]
14. Padin, X.A.; Velo, A.; Pérez, F.F. ARIOS: A Database for Ocean Acidification Assessment in the Iberian Upwelling System (1976–2018). *Earth Syst. Sci. Data* **2020**, *12*, 2647–2663. [CrossRef]
15. Dos Santos, A.; Marques, R.; Pires, R.F.T. Zooplankton Biodiversity and Temporal Dynamics (2005–2015) in a Coastal Station in Western Portugal (Northeastern Atlantic Ocean). *PeerJ* **2023**, *11*, e16387. [CrossRef]
16. Primo, A.L.; Cruz, C.; Martinho, F.; Guerreiro, M.A.; Rodrigues, M.J.; Pardal, M. Climate Forcing on Estuarine Zooplanktonic Production. *Mar. Pollut. Bull.* **2023**, *194*, 115287. [CrossRef] [PubMed]
17. Ranasinghe, R.; Ruane, A.C.; Vautard, R.; Arnell, N.; Coppola, E.; Cruz, F.A.; Dessai, S.; Islam, A.S.; Rahimi, M.; Ruiz Carrascal, D.; et al. Climate Change Information for Regional Impact and for Risk Assessment. In *Climate Change 2021: The Physical Science Basis. Contribution of Working Group I to the Sixth Assessment Report of the Intergovernmental Panel on Climate Change*; Masson-Delmotte, V., Zhai, P., Pirani, A., Connors, S.L., Péan, C., Berger, S., Caud, N., Chen, Y., Goldfarb, L., Gomis, M.I., et al., Eds.; Cambridge University Press: Cambridge, UK; New York, NY, USA, 2021; pp. 1767–1926. [CrossRef]
18. Moss, R.H.; Edmonds, J.A.; Hibbard, K.A.; Manning, M.R.; Rose, S.K.; Van Vuuren, D.P.; Carter, T.R.; Emori, S.; Kainuma, M.; Kram, T.; et al. The next Generation of Scenarios for Climate Change Research and Assessment. *Nature* **2010**, *463*, 747–756. [CrossRef]
19. Gomes, M. Spatial Patterns of Groundfish Assemblages on the Continental Shelf of Portugal. *ICES J. Mar. Sci.* **2001**, *58*, 633–647. [CrossRef]
20. Pecl, G.T.; Hobday, A.J.; Frusher, S.; Sauer, W.H.H.; Bates, A.E. Ocean Warming Hotspots Provide Early Warning Laboratories for Climate Change Impacts. *Rev. Fish Biol. Fish.* **2014**, *24*, 409–413. [CrossRef]
21. Faleiro, F.; Pimentel, M.; Pegado, M.R.; Bispo, R.; Lopes, A.R.; Diniz, M.S.; Rosa, R. Small Pelagics in a Changing Ocean: Biological Responses of Sardine Early Stages to Warming. *Conserv. Physiol.* **2016**, *4*, cow017. [CrossRef]
22. Monteiro, J.N.; Bueno-Pardo, J.; Pinto, M.; Pardal, M.A.; Martinho, F.; Leitão, F. Implications of Warming on the Morphometric and Reproductive Traits of the Green Crab, Carcinus Maenas. *Fishes* **2023**, *8*, 485. [CrossRef]
23. Pinto, M.; Monteiro, J.N.; Crespo, D.; Costa, F.; Rosa, J.; Primo, A.L.; Pardal, M.A.; Martinho, F. Influence of Oceanic and Climate Conditions on the Early Life History of European Seabass Dicentrarchus Labrax. *Mar. Environ. Res.* **2021**, *169*, 105362. [CrossRef]
24. Santos, A. Sardine and Horse Mackerel Recruitment and Upwelling off Portugal. *ICES J. Mar. Sci.* **2001**, *58*, 589–596. [CrossRef]
25. Araújo, J.E.; Madeira, D.; Vitorino, R.; Repolho, T.; Rosa, R.; Diniz, M. Negative Synergistic Impacts of Ocean Warming and Acidification on the Survival and Proteome of the Commercial Sea Bream, Sparus Aurata. *J. Sea Res.* **2018**, *139*, 50–61. [CrossRef]
26. ICES. *Report of the Working Group on Fish Distribution Shifts (WKFISHDISH)*; ICES Expert Group Reports; ICES: Copenhagen, Denmark, 2017. [CrossRef]
27. Caldwell, I.R.; Gergel, S.E. Thresholds in Seascape Connectivity: Influence of Mobility, Habitat Distribution, and Current Strength on Fish Movement. *Landsc. Ecol.* **2013**, *28*, 1937–1948. [CrossRef]
28. Asch, R.G.; Stock, C.A.; Sarmiento, J.L. Climate Change Impacts on Mismatches between Phytoplankton Blooms and Fish Spawning Phenology. *Glob. Change Biol.* **2019**, *25*, 2544–2559. [CrossRef]
29. Cheung, W.W.L.; Watson, R.; Pauly, D. Signature of Ocean Warming in Global Fisheries Catch. *Nature* **2013**, *497*, 365–368. [CrossRef] [PubMed]
30. Leitão, F.; Alms, V.; Erzini, K. A Multi-Model Approach to Evaluate the Role of Environmental Variability and Fishing Pressure in Sardine Fisheries. *J. Mar. Syst.* **2014**, *139*, 128–138. [CrossRef]
31. Pinto, M.; Albo-Puigserver, M.; Bueno-Pardo, J.; Monteiro, J.N.; Teodósio, M.A.; Leitão, F. Eco-Socio-Economic Vulnerability Assessment of Portuguese Fisheries to Climate Change. *Ecol. Econ.* **2023**, *212*, 107928. [CrossRef]
32. Gaspar, M.; Pereira, F.; Martins, R.; Carneiro, M.; Pereira, J.; Moreno, A.; Constantino, R.; Felício, M.; Gonçalves, M.; Viegas, M.d.C.; et al. *Pequena Pesca na Costa Continental Portuguesa: Caracterização Socioeconómica, Descrição da Atividade e Identificação de Problemas*; Instituto Português do Mar e da Atmosfera (IPIMAR): Lisbon, Portugal, 2014; ISBN 978-972-9372-40-7.

33. Cunha, M.E. Physical Control of Biological Processes in a Coastal Upwelling System: Comparison of the Effects of Coastal Topography, River Run-off and Physical Oceanography in the Northern and Southern Parts of the Western Portuguese Coastal Waters. Ph.D. Thesis, Faculty of Sciences, University of Lisbon, Lisbon, Portugal, 2001; 293p.
34. Santos, A.M.P.; Chícharo, A.; Dos Santos, A.; Moita, T.; Oliveira, P.B.; Peliz, Á.; Ré, P. Physical–Biological Interactions in the Life History of Small Pelagic Fish in the Western Iberia Upwelling Ecosystem. *Prog. Oceanogr.* **2007**, *74*, 192–209. [CrossRef]
35. Kay, S. *Marine Biogeochemistry Data for the Northwest European Shelf and Mediterranean Sea from 2006 up to 2100 Derived from Climate Projections*; Copernicus Climate Change Service (C3S), Climate Data Store (CDS): Bonn, Germany, 2020. [CrossRef]
36. Kay, S.; Sailley, S.; Aldridge, J.; McEwan, R.; Talbot, L.; Wilson, R. Technical Report: Validation of Model Datasets Used in Early-Warning System: Climate-Smart Spatial Management of UK Fisheries, Aquaculture and Conservation. 2024. Available online: https://www.mccip.org.uk/sites/default/files/2024-02/5.%20MSPACE_Report_EarlyWarningSystem_Annex1.pdf (accessed on 20 December 2025).
37. Konsta, K.; Doxa, A.; Katsanevakis, S.; Mazaris, A.D. Projected Marine Heatwaves over the Mediterranean Sea and the Network of Marine Protected Areas: A Three-Dimensional Assessment. *Clim. Change* **2025**, *178*, 17. [CrossRef]
38. Zuur, A.F.; Fryer, R.J.; Jolliffe, I.T.; Dekker, R.; Beukema, J.J. Estimating Common Trends in Multivariate Time Series Using Dynamic Factor Analysis. *Environmetrics* **2003**, *14*, 665–685. [CrossRef]
39. Zuur, A.F.; Tuck, I.D.; Bailey, N. Dynamic Factor Analysis to Estimate Common Trends in Fisheries Time Series. *Can. J. Fish. Aquat. Sci.* **2003**, *60*, 542–552. [CrossRef]
40. Zuur, A.F.; Ieno, E.N.; Smith, G.M. *Analysing Ecological Data*; Statistics for Biology and Health; Springer: New York, NY, USA, 2007; ISBN 978-0-387-45967-7.
41. Mann, H.B. Nonparametric Tests Against Trend. *Econometrica* **1945**, *13*, 245–259. [CrossRef]
42. Kendall, M.G. *Rank Correlation Methods*, 4th ed.; Charles Griffin, London—References—Scientific Research Publishing: London, UK, 1975. Available online: https://www.scirp.org/reference/referencespapers?referenceid=2099295 (accessed on 20 May 2026).
43. Sen, P.K. Estimates of the Regression Coefficient Based on Kendall's Tau. *J. Am. Stat. Assoc.* **1968**, *63*, 1379–1389. [CrossRef]
44. Hutchinson, G.E. Concluding Remarks. *Cold Spring Harb. Symp. Quant. Biol.* **1957**, *22*, 415–427. [CrossRef]
45. Soberón, J.; Peterson, A.T. Interpretation of Models of Fundamental Ecological Niches and Species' Distributional Areas. *Biodivers. Inform.* **2005**, *2*, 4. [CrossRef]
46. Peterson, A.T.; Soberón, J.; Pearson, R.G.; Anderson, R.P.; Martínez-Meyer, E.; Nakamura, M.; Araújo, M.B. *Ecological Niches and Geographic Distributions (MPB-49)*; Princeton University Press: Princeton, NJ, USA, 2011; ISBN 978-1-4008-4067-0.
47. Legendre, P.; Legendre, L. *Numerical Ecology*; Elsevier: Amsterdam, The Netherlands, 2012; ISBN 978-0-444-53869-7.
48. Clarke, K.R. Non-Parametric Multivariate Analyses of Changes in Community Structure. *Aust. J. Ecol.* **1993**, *18*, 117–143. [CrossRef]
49. Relvas, P.; Luís, J.; Santos, A.M.P. Importance of the Mesoscale in the Decadal Changes Observed in the Northern Canary Upwelling System. *Geophys. Res. Lett.* **2009**, *36*, 2009GL040504. [CrossRef]
50. Goela, P.C.; Cordeiro, C.; Danchenko, S.; Icely, J.; Cristina, S.; Newton, A. Time Series Analysis of Data for Sea Surface Temperature and Upwelling Components from the Southwest Coast of Portugal. *J. Mar. Syst.* **2016**, *163*, 12–22. [CrossRef]
51. Biguino, B.; Antunes, C.; Lamas, L.; Jenkins, L.J.; Dias, J.M.; Haigh, I.D.; Brito, A.C. 40 Years of Changes in Sea Surface Temperature along the Western Iberian Coast. *Sci. Total Environ.* **2023**, *888*, 164193. [CrossRef]
52. Piedracoba, S.; Pardo, P.C.; Álvarez-Salgado, X.A.; Torres, S. Seasonal, Interannual and Long-Term Variability of Sea Surface Temperature in the NW Iberian Upwelling, 1982–2020. *JGR Ocean.* **2024**, *129*, e2024JC021075. [CrossRef]
53. Bakun, A. Global Climate Change and Intensification of Coastal Ocean Upwelling. *Science* **1990**, *247*, 198–201. [CrossRef]
54. Hurrell, J.W.; Kushnir, Y.; Ottersen, G.; Visbeck, M. An Overview of the North Atlantic Oscillation. *Geophys. Monogr.* **2003**, *134*, 1–36.
55. Santos, A.M.P.; Kazmin, A.S.; Peliz, Á. Decadal Changes in the Canary Upwelling System as Revealed by Satellite Observations: Their Impact on Productivity. *J. Mar. Res.* **2005**, *63*, 359–379. [CrossRef]
56. García-Reyes, M.; Koval, G.; Sydeman, W.J.; Palacios, D.; Bedriñana-Romano, L.; DeForest, K.; Montenegro Silva, C.; Sepúlveda, M.; Hines, E. Most Eastern Boundary Upwelling Regions Represent Thermal Refugia in the Age of Climate Change. *Front. Mar. Sci.* **2023**, *10*, 1158472. [CrossRef]
57. Seabra, R.; Varela, R.; Santos, A.M.; Gómez-Gesteira, M.; Meneghesso, C.; Wethey, D.S.; Lima, F.P. Reduced Nearshore Warming Associated with Eastern Boundary Upwelling Systems. *Front. Mar. Sci.* **2019**, *6*, 104. [CrossRef]
58. Gamito, R.; Pita, C.; Teixeira, C.; Costa, M.J.; Cabral, H.N. Trends in Landings and Vulnerability to Climate Change in Different Fleet Components in the Portuguese Coast. *Fish. Res.* **2016**, *181*, 93–101. [CrossRef]
59. Leitão, F.; Maharaj, R.R.; Vieira, V.M.N.C.S.; Teodósio, A.; Cheung, W.W.L. The Effect of Regional Sea Surface Temperature Rise on Fisheries along the Portuguese Iberian Atlantic Coast. *Aquat. Conserv.* **2018**, *28*, 1351–1359. [CrossRef]
60. Pauly, D. *Gasping Fish and Panting Squids: Oxygen, Temperature and the Growth of Water-Breathing Animals*; International Ecology Institute: Oldendorf/Luhe, Germany, 2010; 279p.

61. Teixeira, C.M.; Gamito, R.; Leitão, F.; Murta, A.G.; Cabral, H.N.; Erzini, K.; Costa, M.J. Environmental Influence on Commercial Fishery Landings of Small Pelagic Fish in Portugal. *Reg. Env. Change* **2016**, *16*, 709–716. [CrossRef]
62. Lima, A.R.A.; Baltazar-Soares, M.; Garrido, S.; Riveiro, I.; Carrera, P.; Piecho-Santos, A.M.; Peck, M.A.; Silva, G. Forecasting Shifts in Habitat Suitability across the Distribution Range of a Temperate Small Pelagic Fish under Different Scenarios of Climate Change. *Sci. Total Environ.* **2022**, *804*, 150167. [CrossRef]
63. Branch, T.A.; DeJoseph, B.M.; Ray, L.J.; Wagner, C.A. Impacts of Ocean Acidification on Marine Seafood. *Trends Ecol. Evol.* **2013**, *28*, 178–186. [CrossRef]
64. Gutiérrez, J.M.; Jones, R.G.; Narisma, G.T.; Alves, L.M.; Amjad, M.; Gorodetskaya, I.V.; Grose, M.; Klutse, N.A.B.; Krakovska, S.; Li, J.; et al. Atlas. In *Climate Change 2021: The Physical Science Basis. Contribution of Working Group I to the Sixth Assessment Report of the Intergovernmental Panel on Climate Change*; Masson-Delmotte, V., Zhai, P., Pirani, A., Connors, S.L., Péan, C., Berger, S., Caud, N., Chen, Y., Goldfarb, L., Gomis, M.I., et al., Eds.; Cambridge University Press: Cambridge, UK; New York, NY, USA, 2021; pp. 1927–2058. [CrossRef]
65. Canadell, J.G. *Ecosystem Collapse and Climate Change*; Ecological Studies; Springer International Publishing AG: Cham, Switzerland, 2021; ISBN 978-3-030-71329-4.
66. IPCC. Sections. In *Climate Change 2023: Synthesis Report. Contribution of Working Groups I, II and III to the Sixth Assessment Report of the Intergovernmental Panel on Climate Change*; Core Writing Team, Lee, H., Romero, J., Eds.; IPCC: Geneva, Switzerland, 2023; pp. 35–115. [CrossRef]
67. Fernandes, J.A.; Papathanasopoulou, E.; Hattam, C.; Queirós, A.M.; Cheung, W.W.W.L.; Yool, A.; Artioli, Y.; Pope, E.C.; Flynn, K.J.; Merino, G.; et al. Estimating the Ecological, Economic and Social Impacts of Ocean Acidification and Warming on UK Fisheries. *Fish Fish.* **2017**, *18*, 389–411. [CrossRef]
68. Garza-Gil, M.D.; Torralba-Cano, J.; Varela-Lafuente, M.M. Evaluating the Economic Effects of Climate Change on the European Sardine Fishery. *Reg. Env. Change* **2011**, *11*, 87–95. [CrossRef]
69. Lozier, M.S.; Dave, A.C.; Palter, J.B.; Gerber, L.M.; Barber, R.T. On the Relationship between Stratification and Primary Productivity in the North Atlantic: Stratification and Primary Productivity. *Geophys. Res. Lett.* **2011**, *38*. [CrossRef]
70. Rhein, M.; Rintoul, S.R.; Aoki, S.; Campos, E.; Chambers, D.; Feely, R.A.; Gulev, S.; Johnson, G.C.; Josey, S.A.; Kostianoy, A.; et al. Observations: Ocean. In *Climate Change 2013: The Physical Science Basis. Contribution of Working Group I to the Fifth Assessment Report of the Intergovernmental Panel on Climate Change*; Stocker, T.F., Qin, D., Plattner, G.-K., Tignor, M., Allen, S.K., Boschung, J., Nauels, A., Xia, Y., Bex, V., Midgley, P.M., Eds.; Cambridge University Press: Cambridge, UK; New York, NY, USA, 2013; pp. 255–316.
71. Cheng, L.; Trenberth, K.E.; Gruber, N.; Abraham, J.P.; Fasullo, J.T.; Li, G.; Mann, M.E.; Zhao, X.; Zhu, J. Improved Estimates of Changes in Upper Ocean Salinity and the Hydrological Cycle. *J. Clim.* **2020**, *33*, 10357–10381. [CrossRef]
72. Santos, A.M.P.; Ré, P.; Dos Santos, A.; Peliz, Á. Vertical Distribution of the European Sardine (Sardina Pilchardus) Larvae and Its Implications for Their Survival. *J. Plankton Res.* **2006**, *28*, 523–532. [CrossRef]
73. Mendes, R.; Sousa, M.C.; deCastro, M.; Gómez-Gesteira, M.; Dias, J.M. New Insights into the Western Iberian Buoyant Plume: Interaction between the Douro and Minho River Plumes under Winter Conditions. *Prog. Oceanogr.* **2016**, *141*, 30–43. [CrossRef]
74. Guerreiro, M.A.; Martinho, F.; Baptista, J.; Costa, F.; Pardal, M.Â.; Primo, A.L. Function of Estuaries and Coastal Areas as Nursery Grounds for Marine Fish Early Life Stages. *Mar. Environ. Res.* **2021**, *170*, 105408. [CrossRef]
75. Garel, E.; Laiz, I.; Drago, T.; Relvas, P. Characterisation of Coastal Counter-Currents on the Inner Shelf of the Gulf of Cadiz. *J. Mar. Syst.* **2016**, *155*, 19–34. [CrossRef]
76. Gerlach, G.; Atema, J.; Kingsford, M.J.; Black, K.P.; Miller-Sims, V. Smelling Home Can Prevent Dispersal of Reef Fish Larvae. *Proc. Natl. Acad. Sci. USA* **2007**, *104*, 858–863. [CrossRef]
77. Downie, A.T.; Illing, B.; Faria, A.M.; Rummer, J.L. Swimming Performance of Marine Fish Larvae: Review of a Universal Trait under Ecological and Environmental Pressure. *Rev. Fish Biol. Fish.* **2020**, *30*, 93–108. [CrossRef]
78. Simpson, S.D.; Piercy, J.J.B.; King, J.; Codling, E.A. Modelling Larval Dispersal and Behaviour of Coral Reef Fishes. *Ecol. Complex.* **2013**, *16*, 68–76. [CrossRef]
79. Teodósio, M.A.; Garrido, S.; Peters, J.; Leitão, F.; Ré, P.; Peliz, A.; Santos, A.M.P. Assessing the Impact of Environmental Forcing on the Condition of Anchovy Larvae in the Cadiz Gulf Using Nucleic Acid and Fatty Acid-Derived Indices. *Estuar. Coast. Shelf Sci.* **2017**, *185*, 94–106. [CrossRef]